

Electronic Supplementary Information (ESI)

**Coordination Compound-Derived Ordered Mesoporous
N-Free Fe-P_x-C Material for Efficient Oxygen
Electroreduction**

Congling. Li, Zhengyan. Chen, Yangyang. Ni, Fantao. Kong, Aiguo. Kong, and
Yongkui. Shan**

*School of Chemistry and Molecular Engineering, East China Normal University, 500
Dongchuan Road, Shanghai 200241, P.R. China.*

E-mail: ykshan@chem.ecnu.edu.cn

Content

Experimental section

Fig. S1. TGA plots of $(\text{Ph}_3\text{P})_2\text{Fe}(\text{CO})_3$ filled SBA-15 in air atmosphere.

Fig. S2. TG and DTA plots of $(\text{Ph}_3\text{P})_2\text{Fe}(\text{CO})_3$ (A) and $(\text{Ph}_3\text{P})_2\text{Fe}(\text{CO})_3$ filled SBA-15 (B) in nitrogen atmosphere.

Fig. S3. (A) N_2 -sorption isotherm curves and (B) the corresponding pore size distribution curves for the SBA-15 before and after introducing the $(\text{Ph}_3\text{P})_2\text{Fe}(\text{CO})_3$.

Fig. S4. XPS survey spectrum for Fe-P-C-900.

Fig. S5. The enlarged FT-IR spectrum for Fe-P-C-900.

Fig. S6. Calibration to reversible hydrogen electrode (RHE)

Fig. S7. RDE polarization curves of Fe-P-C materials and Pt/C at a rotation rate of 400-2500 rpm in an O_2 -saturated 0.1 M KOH solution.

Fig. S8. RDE polarization curves of Fe-P-C materials and Pt/C at a rotation rate of 400-2500 rpm in an O_2 -saturated 0.1 M HClO_4 solution.

Table S1. The surface composition and the relative content of different types of doped nitrogen estimated from the XPS analysis.

Table S2. The physical parameters of the SBA-15 before and after introducing the $(\text{Ph}_3\text{P})_2\text{Fe}(\text{CO})_3$.

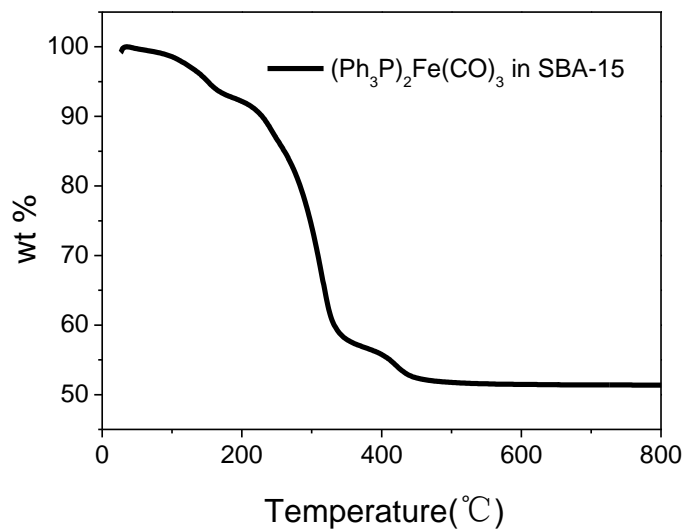
References

Experimental section

Preparation of SBA-15

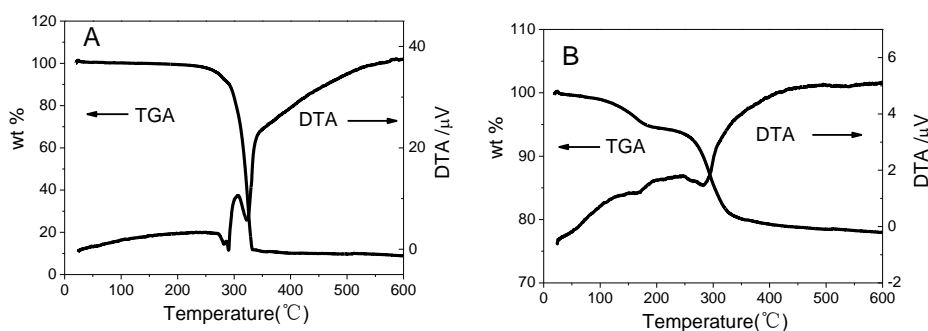
In the typical preparation, P123 (4.0 g, $M_w = 5800$, Aldrich) was completely dissolved in a solution containing deionized (DI) water (144 g) and HCl (160 ml, 1.6 M) under stirring at 40 °C. Then, tetraethyl orthosilicate (8.3 g) was added in and stirred at 40 °C for 24 h. The obtained mixtures were transferred to a Teflon-lined autoclave and then, heated at 150 °C for 24 h. The resulting white precipitates were filtered, washed with DI water, and dried at 100 °C for 24 h. Finally, after it was further calcined at 550 °C in air for 4 h with heating rate of 1 °C min⁻¹, mesoporous SBA-15 silica was obtained.

Fig. S1. TGA plots of $(\text{Ph}_3\text{P})_2\text{Fe}(\text{CO})_3$ filled SBA-15 in air atmosphere.



It can be seen from this TGA plot, a small weight loss of ~8 % between 20-150 °C corresponding to the loss of the adsorbed H_2O in the mesopore of SBA-15, followed by ~40 % weight loss during the temperature range of 150-450 °C corresponding to the pyrolysis of $(\text{Ph}_3\text{P})_2\text{Fe}(\text{CO})_3$ and no further weight loss when temperature reached to 800 °C.

Fig. S2. TG and DTA plots of $(\text{Ph}_3\text{P})_2\text{Fe}(\text{CO})_3$ (A) and $(\text{Ph}_3\text{P})_2\text{Fe}(\text{CO})_3$ filled SBA-15 (B) in nitrogen atmosphere.



The carbonization behavior of $(\text{Ph}_3\text{P})_2\text{Fe}(\text{CO})_3$ has been investigated by TG-DTA in nitrogen atmosphere (200 ml/min) with a heating rate of 10 °C/min. For the $(\text{Ph}_3\text{P})_2\text{Fe}(\text{CO})_3$ sample, as indicated by DTA curve (Fig. S2A), the endothermic peak at around 270 °C corresponds to the melting point of the $(\text{Ph}_3\text{P})_2\text{Fe}(\text{CO})_3$ compound that is immediately followed by another endothermic peak at around 330 °C, which is associated with weight loss between 260 and 340 °C as observed from the TGA curve. Prolonged heating to 600 °C does not produce any significant endothermic or exothermic peaks on DTA curve, the final thermal decomposition residue is about 10 wt. %. While the $(\text{Ph}_3\text{P})_2\text{Fe}(\text{CO})_3$ encapsulated in mesoporous channels of SBA-15 hard templates, it can be seen in Fig. S2B that the endothermic peak on DTA curve at around 160 °C corresponds to the desorption of H_2O , which is associated with 8 % weight loss between 20 and 160 °C as observed from the TGA curve. Another endothermic peak at around 300 °C is associated with 14 % weight loss between 260 and 340 °C as observed from the TGA curve, corresponding to the pyrolysis of $(\text{Ph}_3\text{P})_2\text{Fe}(\text{CO})_3$. No further obvious weight loss when temperature reached to 600 °C, but the result in the Fig.S1 indicates that percentage of $(\text{Ph}_3\text{P})_2\text{Fe}(\text{CO})_3$ in the filled SBA-15 is determined to be about 43 wt. % by TGA analysis in air atmosphere (Fig. S1), it suggests that the utilization of SBA-15 silica hard templates remarkably prevent $(\text{Ph}_3\text{P})_2\text{Fe}(\text{CO})_3$ from decomposing or evaporating and facilitated the carbonization of $(\text{Ph}_3\text{P})_2\text{Fe}(\text{CO})_3$ encapsulated in mesoporous channels of hard templates.

Fig. S3. (A) N_2 -sorption isotherm curves and (B) the corresponding pore size distribution curves for the SBA-15 before and after introducing the $(Ph_3P)_2Fe(CO)_3$.

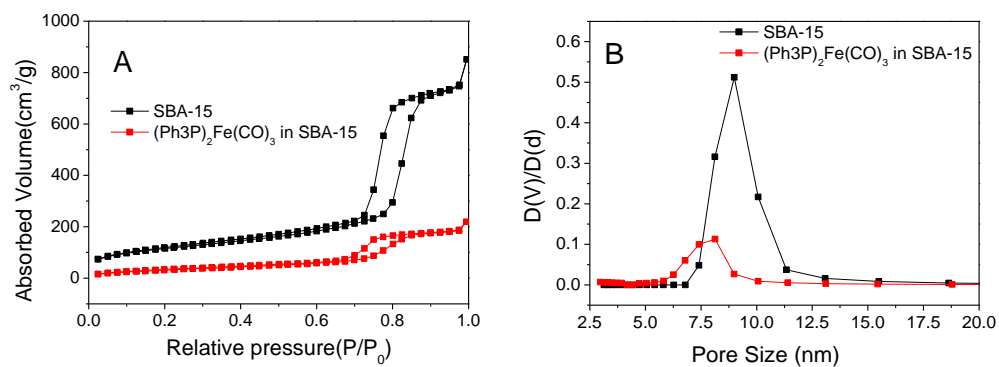


Fig. S4. XPS survey spectrum for Fe-P-C-900.

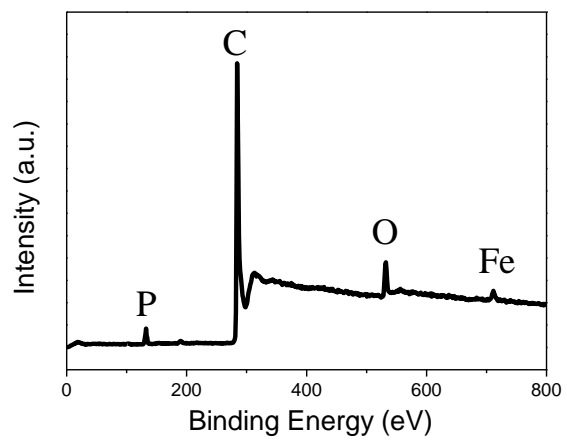


Fig. S5. The enlarged FT-IR spectrum for Fe-P-C-900.

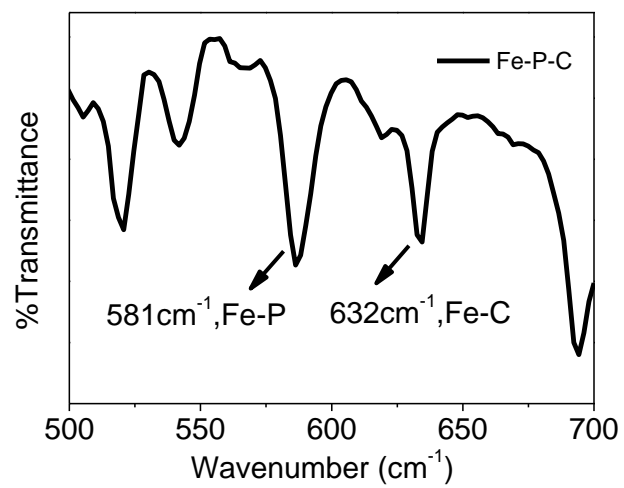


Fig. S6. Calibration to reversible hydrogen electrode (RHE).

Ag/AgCl (3.5 M, KCl) electrode using as the reference electrode in all our measurements was calibrated with respect to RHE. In H₂-saturated electrolyte, while the platinum wires was used as the working electrode and the counter electrode, the crossing potential at zero current was taken to be the potential for the reaction of H⁺/H₂ reaction. Using these crossing potential in either 0.1M KOH or 0.1 M HClO₄ electrolytes, all the reported potentials were calibrated to the RHE potentials according to the reported method^{S1}.

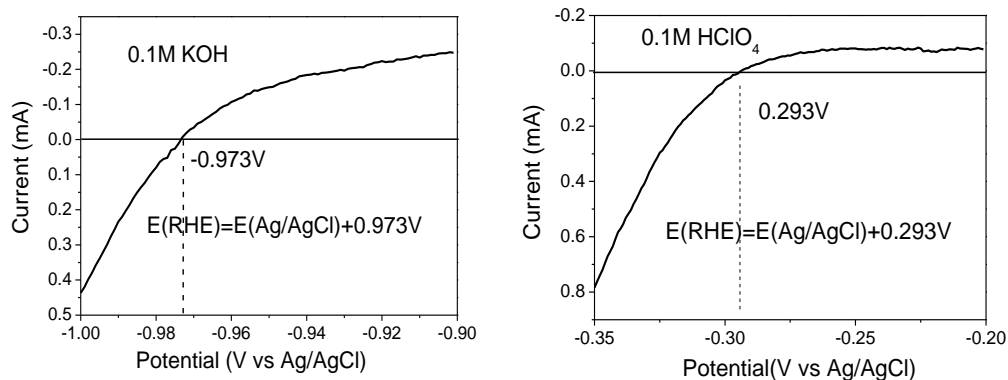


Fig. S7. RDE polarization curves of Fe-P-C materials and Pt/C at a rotation rate of 400-2500 rpm in an O₂-saturated 0.1 M KOH solution.

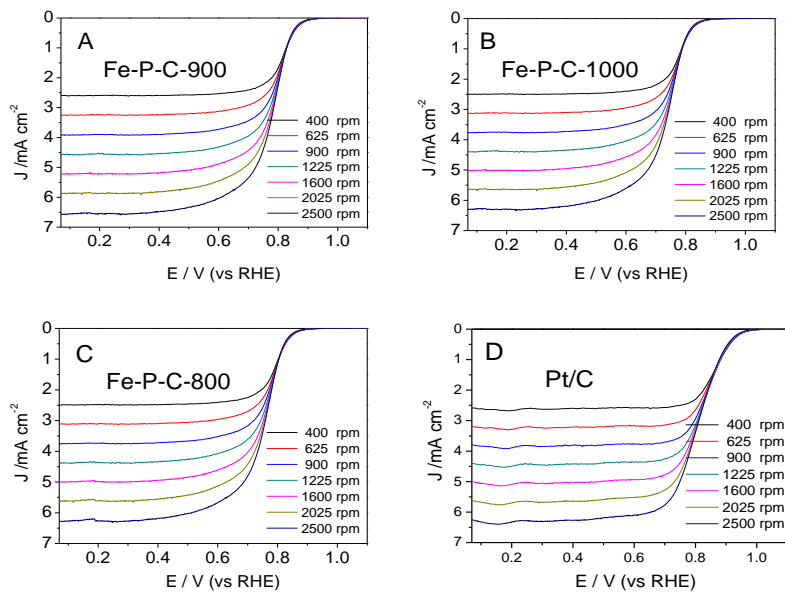


Fig. S8. RDE polarization curves of Fe-P-C materials and Pt/C at a rotation rate of 400-2500 rpm in an O₂-saturated 0.1 M HClO₄ solution.

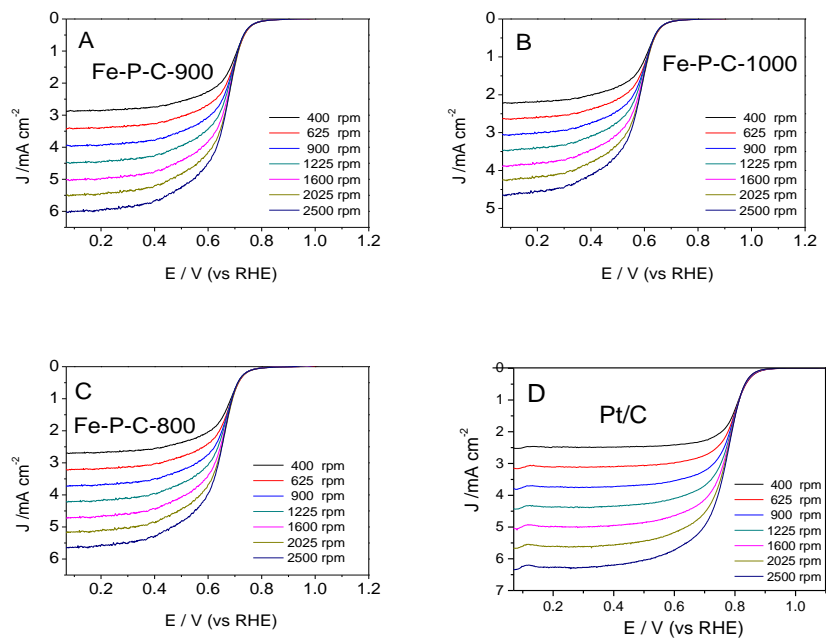


Table S1. The surface composition and the relative content of different types of doped nitrogen estimated from the XPS analysis.

Samples	Fe (at %)	P (at %)	C (at %)	O (at %)	P-C (%)	P-O (%)
Fe-P-C-800	1.4	4.1	82.1	12.4	63.5	36.5
Fe-P-C-900	1.2	3.8	83.8	11.2	70.1	29.9
Fe-P-C-1000	0.9	2.9	86.7	9.5	9.5	46.4

Table S2. The physical parameters of the SBA-15 before and after introducing the $(\text{Ph}_3\text{P})_2\text{Fe}(\text{CO})_3$.

Samples	Surface area ($\text{m}^2 \text{g}^{-1}$)	Pore size (nm)	Pore volume ($\text{cm}^3 \text{g}^{-1}$)
SBA-15	506	8.9	1.37
$(\text{Ph}_3\text{P})_2\text{Fe}(\text{CO})_3$ in SBA-15	147	8.1	0.34

S1 J.Y. Cheon, T. Kim, Y.M. Choi Y M, *Scientific reports*, 2013, **3**. 2715